Hydrogen-Induced Surface Metallization of $SrTiO_3(001)$

M. D'Angelo,[1,*] R. Yukawa,[2] K. Ozawa,[3] S. Yamamoto,[2] T. Hirahara,[4] S. Hasegawa,[4] M. G. Silly,[5] F. Sirotti,[5] and I. Matsuda[2]

[1]*Institut des Nanosciences de Paris, Université Pierre et Marie Curie-Paris 6, CNRS-UMR 7588, 4 place Jussieu, 75252 Paris, France*
[2]*Institute for Solid State Physics, University of Tokyo, Kashiwa, Chiba 277-8581, Japan*
[3]*Department of Chemistry and Materials Science, Tokyo Institute of Technology, 2-12-1 Ookayama, Meguro-ku, Tokyo 152-8551, Japan*
[4]*Department of Physics, School of Science, University of Tokyo, 7-3-1 Hongo, Bunkyo-ku, Tokyo 113-0033, Japan*
[5]*TEMPO Beamline, Synchrotron Soleil, L'Orme des Merisiers Saint-Aubin, B.P. 48, 91192 Gif-sur-Yvette Cedex, France*

(Received 3 November 2011; published 16 March 2012)

Surface metallization of $SrTiO_3(001)$ by hydrogen adsorption is experimentally confirmed for the first time by photoemission spectroscopy and surface conductivity measurements. The metallic state is assigned to a quantized state in the space-charge layer induced by electron doping from hydrogen atoms. The measured two-dimensional (2D) conductivity is well above the 2D Ioffe-Regel limit indicating that the system is in a metallic conduction regime. The mean free path of the surface electron is estimated to be several nanometers at room temperature.

DOI: 10.1103/PhysRevLett.108.116802 PACS numbers: 73.25.+i

Transition-metal oxides and especially perovskite-type oxides have been extensively studied in the past decades for their large range of intrinsic properties such as superconductivity, magnetoresistance, or ferroelectricity. Until recently, it was believed that due to their chemical complexity these oxides could not be used for oxide-based electronics. However, it is now widely admitted that oxide materials devices not only can meet the standards of the semiconductor-based electronics but additionally show new intriguing properties due to electron correlations [1]. Among these oxides, $SrTiO_3$ appears as a key material for this new emerging field of all-oxide electronics [2,3]. A first breakthrough was achieved with the discovery of a two-dimensional electron gas at the interface of the two insulating oxides $LaAlO_3$ and $SrTiO_3$ [4]. This system focused a great interest, and further studies revealed that this interface shows not only high mobility electron gas [5] but also large magnetoresistance [6] and even superconductivity [7]. Yet, the detailed mechanisms giving rise to the conductivity at the interface are still not understood. Proposed explanations involve different processes at the interface such as La diffusion [8], oxygen vacancies [9,10], or electronic reorganization to avoid polar catastrophe [11]. Moreover, recent angle-resolved photoemission studies evidenced a highly metallic universal two-dimensional electron gas at the vacuum-cleaved $SrTiO_3$ (STO) surface, suggesting that the properties of STO surface itself might actually play a crucial role in the metallization of the $LaAlO_3/SrTiO_3$ interface [12,13]. Difficulty in the interpretation is partly due to sample preparation of the oxide surface or interface. As mentioned, preparation of heterojunctions or crystal cleavage are associated with possible diffusion of metal atoms and creation of oxygen vacancies.

On the other hand, it has been predicted recently by *ab initio* calculations that hydrogen adsorption on a SrO- or TiO_2-terminated $SrTiO_3(001)$ surface leads to a metallic state at the surface [14]. Such H-induced metallization was already reported for H/ZnO [15] and H/β-SiC [16] crystal surfaces. In the case of $SrTiO_3$ surface, the metallicity is assigned to the bulk-band bending near the surface, where the bulk conduction band is filled with electrons donated from the H atoms on the surface [14]. As hydrogen adsorption on a crystal surface prepared under UHV is a well-controlled procedure, experimental examination of the H-induced metallization of a $SrTiO_3(001)$ surface is thus strongly called for.

For the present Letter, we performed both photoemission and transport experiments on the $H/SrTiO_3(001)$ system. We find a dispersing metallic band and an increase of the surface conductivity after H adsorption. The metallic state is assigned to a quantized state in the space-charge layer near the surface. After the metallization, an electronic state is found in the bulk-band gap [in-gap state (IGS)], and a state, assigned to the O-H bond, is also observed. The measured two-dimensional (2D) conductivity exceeds the 2D Ioffe-Regel limit, indicating the band conduction regime, and the mean free path of surface electrons is estimated to be several nanometers at room temperature.

The electronic structure of the clean and H-adsorbed $SrTiO_3(001)$ surfaces is investigated by core-level and valence band photoemission spectroscopy measurements at the TEMPO beam line, Soleil, France [17], and SPring-8 BL07LSU. The measurements were performed with linearly polarized light, under ultrahigh vacuum (UHV) conditions (base pressure of 4×10^{-10} mbar), at room and low (20 K) temperature. The energy and angle resolution are 60 meV and 0.3°, respectively. Electrical conductivity is

measured *in situ* during H exposure by the four-terminal method under UHV conditions with linearly aligned four probes. Details of the experimental system are described elsewhere [18,19].

We used *n*-type $SrTiO_3(001)$ wafers (0.05 wt % Nb-doped). Before introduction into the UHV chambers, the wafers were treated with buffered HF solution (pH $\sim$ 3.5) for 30 s, followed by rinsing with distilled water. This process is known to leave the (001) surface terminated by a TiO_2 plane [20]. A clean $SrTiO_3(001)$ surface was prepared by heat treatment at 600 °C under 6×10^{-6} mbar of oxygen gas (99.999% purity) in the UHV chamber. In these conditions, a high-quality bulk truncated ordered surface is obtained as confirmed by observation of a sharp 1×1 pattern in low-energy electron diffraction. Negligible carbon contamination and the absence of Sr segregation or oxygen vacancies was ascertained by observation of C 1*s*, Sr 3*d*, Ti 2*p*, and O 1*s* core-level photoemission spectra, respectively [21].

The $SrTiO_3(001)$ surface is exposed to atomic hydrogen, by cracking hydrogen molecules with a hot tungsten filament. No change of the photoemission peak position or surface conductivity is observed by exposing the sample to hydrogen molecules. Since the dissociation rate of hydrogen molecules and the adsorption probability of hydrogen atoms depend on the experimental setups, the results for the H-covered surfaces showing saturation of the photoemission peak shift and of the conductivity change are referred to as "H-saturated" $SrTiO_3(001)$ surfaces.

Figure 1(a) shows photoemission spectra near the Fermi level for the clean surface, intermediate, and the saturation hydrogen coverage taken at $h\nu = 81$ eV. For the clean surface, no state is observed at the Fermi level, indicating its insulating behavior. With the hydrogen exposure, a sharp photoemission signal, denoted as the metallic state (MS), develops at the Fermi level. The H-saturated surface is metallic, and thus the $SrTiO_3(001)$ crystal exhibits a surface insulator-to-metal transition or surface metallization by hydrogen adsorption. On the hydrogenated surface, an electronic state, located within the bulk-band gap of $SrTiO_3(001)$, is observed at a binding energy of 1.5 eV. This IGS has been reported in previous photoemission studies on electron-doped $SrTiO_3(001)$ crystals [22]. The origin of the IGS has been argued by various models: It has been attributed to a locally screened incoherent state of the Ti 3*d*-O 2*p* band [22], a precursor of the "lower-Hubbard band" of the d^1 insulator [23], chemical disorder [24], and the polaron effect [25]. Observation of the IGS on the well-defined surface in the present research seems to deny a chemical origin such as an oxygen vacancy state. Valence band photoemission spectra before and after hydrogen exposure, in Fig. 1(b), show also the appearance of a new state, assigned to the O-H bond. The hydrogen atoms likely adsorb on the oxygen sites, as predicted by first-principles calculations [14].

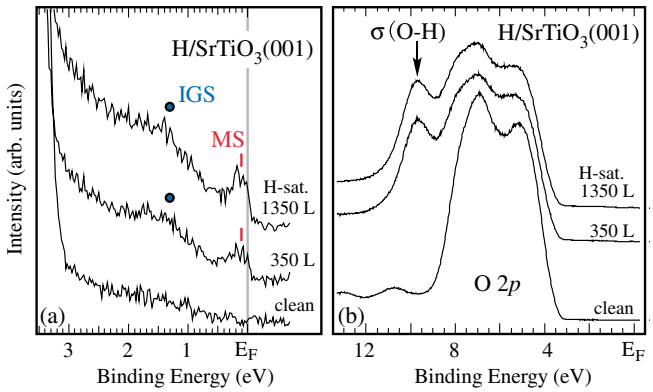

FIG. 1 (color online). Normal-emission angle-integrated photoemission spectra of the bare, H-covered (intermediate coverage) and H-saturated $SrTiO_3(001)$ surfaces (a) at the Fermi level (E_F) and (b) at the O 2*p* band. Spectra were taken at $h\nu =$ 81 eV and at room temperature. MS indicates the position of the metallic state and IGS of the in-gap state.

Figure 2(a) shows wave-number-resolved photoemission spectra of the H-saturated $SrTiO_3(001)$ surface around the $\overline{\Gamma}$ point. Two main features can be observed: a sharp peak denoted MS and a broader feature at around 200 meV. Figure 2(c) displays the second derivative of the photoemission intensity. Whereas MS appears as a sharp peak, the state at 200 meV shows a broad feature. This might

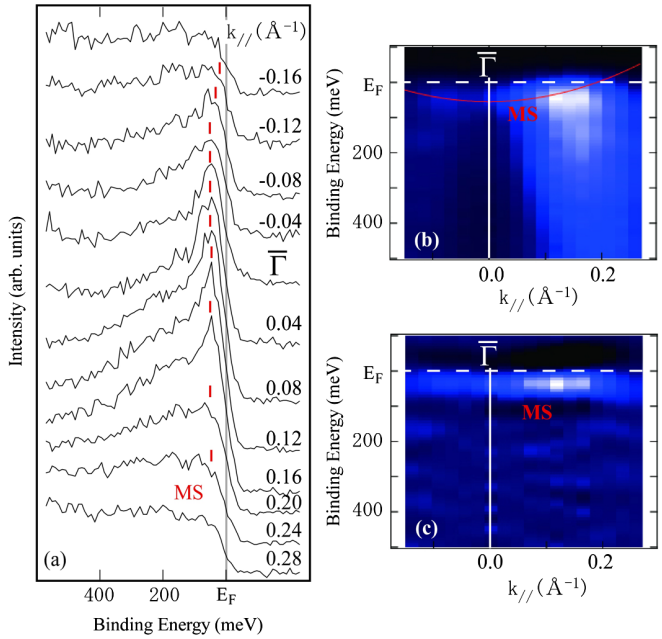

FIG. 2 (color online). (a) Wave-number-resolved photoemission spectra of the H-saturated (1350 L) $SrTiO_3(001)$ surface along the $\overline{\Gamma}$-$\overline{X}$ direction, taken at $h\nu = 81$ eV and at 20 K. (b) Color-scale image of the photoemission intensity. (c) Second derivative of the photoemission intensity. MS denotes the metallic state position. The red line indicates the parabolic fit for the metallic state. Color scale: Black (minimum intensity) to white (maximum of intensity).

indicate that, whereas the MS band is a coherent state, the broad feature can be attributed to an incoherent state due to the electron correlation effect [13,26] or electron-phonon interaction [27]. The MS band shows band dispersion with the band minimum at $\overline{\Gamma}$ and the Fermi wave number of $k_F = 0.2$ Å^{-1}. A parabolic fit of the band dispersion gives an effective mass of $m^*/m_0 = 2.5$, where m_0 is the free electron mass [Fig. 2(b)]. From the k_F value, the carrier density can be deduced to $n_{2D} = 6 \times 10^{13}$ cm^{-2}, which in turn gives around 0.1 electron per unit cell.

To evaluate the bulk-band change, Ti $2p$ core-level photoemission spectra are measured before and after the H exposure, as shown in Fig. 3. The Ti $2p$ peak shifts by 200 meV toward higher binding energies after H adsorption.

From the valence band photoemission spectra on the clean surface (Fig. 1), the valence band maximum position is deduced to be around 3.1 eV below the Fermi level. Thus, the edge of the bulk conduction band is likely located around 100 meV above E_F for the clean $SrTiO_3(001)$ surface. After H deposition, by taking into account a 200 meV downwards band bending, the conduction band minimum is located approximatively 100 meV below the Fermi level, lower than the minimum of the metallic state. The MS state is thus attributed to a quantized state due to confinement in the potential well of the space-charge layer [12]. The sample doping level is 10^{19} cm^{-3}. Taking for the conduction and valence band density of states $N_C(T) = 4.1 \times 10^{16} T^{3/2}$ cm^{-3} and $N_V(T) = 2.5 \times 10^{16} T^{3/2}$ cm^{-3}, respectively [28], we found, from standard semiconductor equations, that in the bulk STO the Fermi level is located 80 meV under the conduction band minimum at room temperature. This means that on the clean surface the bands are bent upwards. The bulk-band-bending change by H adsorption on $SrTiO_3(001)$ is schematically drawn in Fig. 4. With increasing H exposure, the conduction band is progressively filled with electrons from the hydrogen adatoms, and the consequent downward shifts lead eventually to the surface metallization.

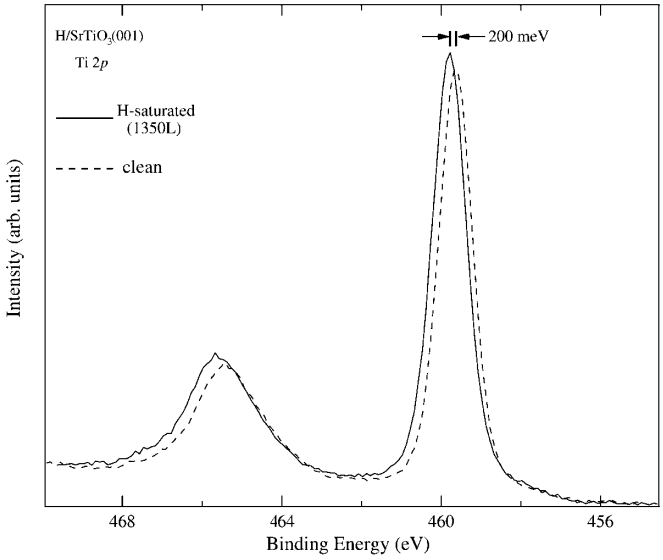

FIG. 3. Ti$2p$ core-level photoemission spectra of the clean and H-saturated $SrTiO_3(001)$ surfaces at room temperature. The photon energy is $h\nu = 605$ eV.

The insulator-to-metal transition at the surface indicates an increase of the conductivity by hydrogen adsorption on the $SrTiO_3(001)$ surface. To correlate with the changes in electronic structures observed by photoemission, surface conductivity measurements are performed for the $H/SrTiO_3(001)$ system. The experimental setup is schematically drawn in Fig. 5(a). The probe distance is ~6 mm, which provides enough area between probes to make *in situ* transport measurement during the H adsorption on the surface [18,19].

Figure 5(b) shows the sheet conductivity change $\Delta\sigma$ of the $SrTiO_3(001)$ surface as a function of H exposure. The $\Delta\sigma$ value is derived from the measured electrical resistance R by the relation $\Delta\sigma = \frac{L}{W}(\frac{1}{R} - \frac{1}{R_0})$, where L and W represent the length (8 mm) and width (5 mm), respectively, of the measured area. R_0 is the initial resistance of the clean surface, and R the resistance of the surface after H deposition.

The transport results in Fig. 5 reveal an increase of the conductivity by the H adsorption. H adsorption is associated with changes only at the space-charge layer, and there is no transport variation in the internal bulk. Since the largest contribution originates from an increase of carriers in the accumulation layers, as shown in Fig. 4, $\Delta\sigma$ after the saturation, $\Delta\sigma_{sat} = 440\ \mu$S/□, corresponds to the conductivity of the H-saturated $SrTiO_3(001)$ surface, $\Delta\sigma_{sat} = \sigma_{H/STO}$.

The conductivity measured on the H-saturated $SrTiO_3(001)$ surface indicates that the electron transport is in the metallic conduction regime. Indeed, electron transport is in the metallic conduction regime if conductivity exceeds the 2D Ioffe-Regel (2D-IR) limit

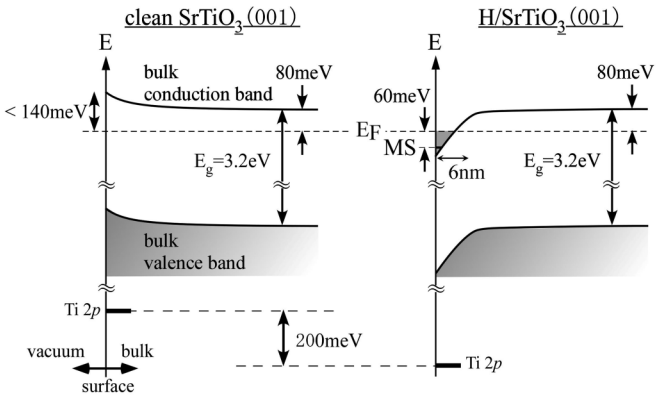

FIG. 4. Schematic drawing of the band-bending change induced by surface metallization during hydrogen adsorption on the $SrTiO_3(001)$ surface. The Debye length is estimated to 6 nm.

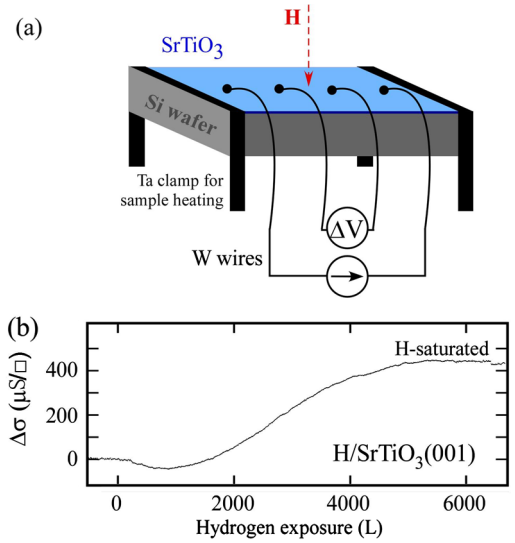

FIG. 5 (color online). (a) Schematic of four-terminal method transport measurements on the $H/SrTiO_3(001)$ surface. (b) Conductivity change $\Delta\sigma$ with H exposure, referred to the conductivity of the clean surface. Measurements were performed at room temperature.

$\sigma_{2D\text{-}IR} = (e^2/h)(k_F l) = (e^2/h)(1) = 39\ \mu S$, where k_F and l are the Fermi wave number and carrier mean free path, respectively. In contrast, electron transport is in the hopping or strong localization regime if conductivity is smaller than $\sigma_{2D\text{-}IR}$. Since $\sigma_{H/STO}$ is much larger than $\sigma_{2D\text{-}IR}$, the measured conductivity is in the band conduction regime, and the increase agrees with the band-bending scenario in Fig. 4.

In addition, the electron mean free path of the H-saturated $SrTiO_3(001)$ surface is derived to be $l \sim 2$ nm from the isotropic 2D Boltzmann equation [29] $\sigma_{H/STO} = (e^2/h)(k_F l)$. The relaxation time $\tau = l/vF$ is thus $\tau = 7.5 \times 10^{-15}$ s, which is similar to those (10^{-15} s) evaluated from resistivity of Nb-doped $SrTiO_3$ crystals at room temperature [30] through the Drude model. The conduction process at room temperature is generally dominated by electron-phonon interaction. In the high temperature limit ($T > T_D/3$ with $T_D = 413$ K being the Debye temperature for $SrTiO_3$ [31]), τ is given by $\tau \sim \tau_{e\text{-ph}} = \hbar/2\pi\lambda k_B T$ with λ representing the strength of the electron-phonon coupling. From our experimental τ value, $\lambda = 0.5$ is obtained, which is comparable to the value from previous photoemission research on the cleaved $SrTiO_3$ surface [32].

In summary, through photoemission spectroscopy and transport measurements on the $SrTiO_3(001)$-(1×1) surface, we evidenced an insulator-to-metal transition induced by hydrogen adsorption. The surface metallization is due to electron doping into the conduction band which shifts under the Fermi level with the appearance of a quantized state in the space-charge layer. The value of the surface conductivity and derived mean free path show that the system is in the metallic conduction regime. These results open up the possibilities of designing future devices of perovskite oxides and of extending to much detailed studies on their carrier dynamics.

Hiroshi Kumigashira is acknowledged for providing sample wafers. Mikk Lippmaa, Seiji Kawasaki, Satoshi Kitagawa, and Hiroshi Daimon are gratefully acknowledged for their valuable support in the experiment. This work was performed by using facilities of the Synchrotron Soleil, France, and Synchrotron Radiation Research Organization, the University of Tokyo (Proposal No. 7401 for 2009–2011 and No. 2011A7415). This work was partly supported by PICS/CNRS and by JSPS.

*dangelo@insp.jussieu.fr

[1] H. Takagi and H. Y. Hwang, Science **327**, 1601 (2010).
[2] C. Cen, S. Thiel, J. Mannhart, and J. Levy, Science **323**, 1026 (2009).
[3] A. P. Ramirez, Science **315**, 1377 (2007).
[4] A. Ohtomo, D. A. Muller, J. L. Grazul, and H. Y. Hwang, Nature (London) **419**, 378 (2002).
[5] A. Ohtomo and H. Y. Hwang, Nature (London) **427**, 423 (2004).
[6] A. Brinkman, M. Huijben, M. van Zalk, J. Huijben, U. Zeitler, J. C. Maan, W. G. van der Wiel, G. Rijnders, D. H. A. Blank, and H. Hilgenkamp, Nature Mater. **6**, 493 (2007).
[7] N. Reyren *et al.*, Science **317**, 1196 (2007).
[8] P. R. Willmott *et al.*, Phys. Rev. Lett. **99**, 155502 (2007).
[9] A. Kalabukhov, R. Gunnarsson, J. Borjesson, E. Olsson, T. Claeson, and D. Winkler, Phys. Rev. B **75**, 121404 (2007).
[10] W. Siemons, G. Koster, H. Yamamoto, W. A. Harrison, G. Lucovsky, T. H. Geballe, D. H. A. Blank, and M. R. Beasley, Phys. Rev. Lett. **98**, 196802 (2007).
[11] N. Nakagawa, H. Y. Hwang, and D. A. Muller, Nature Mater. **5**, 204 (2006).
[12] A. F. Santander-Syro *et al.*, Nature (London) **469**, 189 (2011).
[13] W. Meevasana, P. D. C. King, R. H. He, S.-K. Mo, M. Hashimoto, A. Tamai, P. Songsiriritthigul, F. Baumberger, and Z.-X. Shen, Nature Mater. **10**, 114 (2011).
[14] F. Lin, S. Wang, F. Zheng, G. Zhou, J. Wu, B.-L. Gu, and W. Duan, Phys. Rev. B **79**, 035311 (2009).
[15] K. Ozawa and K. Mase, Phys. Rev. B **81**, 205322 (2010).
[16] V. Derycke, P. G. Soukiassian, F. Amy, Y. J. Chabal, M. D. D'Angelo, H. B. Enriquez, and M. G. Silly, Nature Mater. **2**, 253 (2003).
[17] F. Polack *et al.*, AIP Conf. Proc. **1234**, 185 (2010).
[18] S. Hasegawa and S. Ino, Phys. Rev. Lett. **68**, 1192 (1992).
[19] M. D'Angelo, K. Takase, N. Miyata, T. Hirahara, S. Hasegawa, A. Nishide, M. Ogawa, and I. Matsuda, Phys. Rev. B **79**, 035318 (2009).
[20] T. Nishimura, A. Ikeda, H. Namba, T. Morishita, and Y. Kido, Surf. Sci. **421**, 273 (1999).

[21] D. Kobayashi *et al.*, J. Appl. Phys. **96**, 7183 (2004).
[22] Y. Ishida, R. Eguchi, M. Matsunami, K. Horiba, M. Taguchi, A. Chainani, Y. Senba, H. Ohashi, H. Ohta, and S. Shin, Phys. Rev. Lett. **100**, 056401 (2008).
[23] A. Fujimori, I. Hase, H. Namatame, Y. Fujishima, Y. Tokura, H. Eisaki, S. Uchida, K. Takegahara, and F. M. F. de Groot, Phys. Rev. Lett. **69**, 1796 (1992).
[24] D. D. Sarma, S. R. Barman, H. Kajueter, and G. Kotliar, Europhys. Lett. **36**, 307 (1996).
[25] A. Fujimori, K. K. K. Bocquet, A. E. Morikawa, T. Saitoh, Y. Tokura, I. Hase, and M. Onoda, J. Phys. Chem. Solids **57**, 1379 (1996).
[26] M. Imada, A. Fujimori, and Y. Tokura, Rev. Mod. Phys. **70**, 1039 (1998).
[27] Y. J. Chang, A. Bostwick, Y. S. Kim, K. Horn, and E. Rotenberg, Phys. Rev. B **81**, 235109 (2010).
[28] R. Moss, Ph.D. thesis, Karlsruhe University, 1994.
[29] I. Matsuda, T. Hirahara, M. Konishi, C. Liu, H. Morikawa, M. D'Angelo, S. Hasegawa, T. Okuda, and T. Kinoshita, Phys. Rev. B **71**, 235315 (2005).
[30] A. Spinelli, M. A. Torija, C. Liu, C. Jan, and C. Leighton, Phys. Rev. B **81**, 155110 (2010).
[31] W. N. Lawless, Phys. Rev. B **17**, 1458 (1978).
[32] W. Meevasana *et al.*, New J. Phys. **12**, 023004 (2010).